

Investigation into liquid crystalline smectic- C^* subphase stability using chiral and achiral dopants

J. Kirchhoff and L. S. Hirst*

MARTECH, Department of Physics, Florida State University, Florida 32306, USA

(Received 24 May 2007; published 9 November 2007)

In this paper we investigate the influence of chiral and achiral dopants on a chiral smectic liquid crystal material, which exhibits a rich phase sequence, including the antiferroelectric phase and the three-layer intermediate smectic ($\text{SmC}_{\text{FI1}}^*$) phase. Using polarized optical microscopy, differential scanning calorimetry, and x-ray diffraction we find that small amounts of achiral dopant have the ability to significantly broaden the $\text{SmC}_{\text{FI1}}^*$ phase, whereas an oppositely-handed dopant (otherwise identical to the host material) destabilizes the phase. This work clearly indicates that bulk chirality strongly influences $\text{SmC}_{\text{FI1}}^*$ phase formation and that steric effects also play an important role. Interestingly, addition of the shorter achiral molecule (8CB) was observed to increase the smectic layer spacing, most likely by suppressing interdigitation of alkyl chains between adjacent smectic layers. Control of the $\text{SmC}_{\text{FI1}}^*$ phase width using mixtures in this way is clearly important for effective phase characterization, and could potentially lead to commercially viable materials with a stable $\text{SmC}_{\text{FI1}}^*$ phase over a large temperature range.

DOI: 10.1103/PhysRevE.76.051704

PACS number(s): 64.70.Md, 61.10.Eq, 61.30.Cz

I. INTRODUCTION

In recent years a significant amount of effort in liquid crystal research has been devoted to the characterization of the chiral smectic- C (SmC^*) subphases, both by x-ray diffraction techniques and electro-optical methods [1–3]. This family of liquid crystal phases is important both for theoretical reasons (the phases show ferroelectric, antiferroelectric, and ferroelectriclike properties without long-range order) and also experimentally. If commercially viable compounds and mixtures can be developed then the subsequent new materials could potentially provide a significant leap forward in the functionality of the now ubiquitous liquid crystal display.

The different smectic liquid crystal phases are each composed of similar layered arrangements of molecules, with fluidlike ordering in the plane of the layer. Each variant phase is distinguished by the orientation of the molecules within a certain layer with respect to that in the adjacent layers. One can describe the structure of each SmC^* subphase by the use of the diagrams presented in Fig. 1. A single molecule can be represented as lying on the side of an imaginary cone [Fig. 1(e)], the axis of the cone being parallel to the layer normal \hat{n} . The azimuthal angle φ changes differently from layer to layer in each phase and this is illustrated in Figs. 1(a)–1(d). Notice how in addition to the layer to layer changes there is also an overall precession in φ due to the chirality of the phase. This slow precession gives rise to the macroscopic pitch of the material.

The smectic- C^* subphases have recently become a focus of calamitic liquid crystal research because of their electro-optical properties and their potential for applications [4–6]. Although to date commercial switchable devices have only been manufactured from the ferroelectric (SmC^*) phase, the antiferroelectric (SmC_A^*) phase also shows potential for analog grey scale along with V shaped switching materials [7].

Two additional sub-phases are the $\text{SmC}_{\text{FI1}}^*$ and $\text{SmC}_{\text{FI2}}^*$ phases, also known as the intermediate phases. Experiments have shown that the $\text{SmC}_{\text{FI1}}^*$ phase is a chiral liquid crystal phase with a three-layer clock structure, while the $\text{SmC}_{\text{FI2}}^*$ phase exhibits a four-layer clock structure [8,9]. In addition, more recent work using high resolution resonant x-ray diffraction demonstrated that both the “four-layer phase” ($\text{SmC}_{\text{FI2}}^*$) and the “three-layer phase” ($\text{SmC}_{\text{FI1}}^*$) have a “distorted” clock structure, as can be seen in Figs. 1(c) and 1(d)

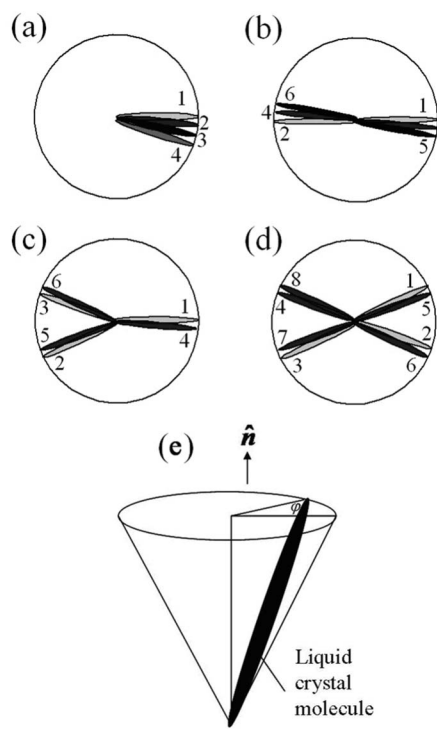


FIG. 1. Cartoon illustrating the periodic clock structures of the (a) SmC^* , (b) SmC_A^* , (c) $\text{SmC}_{\text{FI1}}^*$, (d) $\text{SmC}_{\text{FI2}}^*$ phases and (e) a schematic showing the geometry of a single liquid crystal molecule.

*Author to whom correspondence should be addressed.

[10,11]. The $\text{SmC}^*_{\text{FI1}}$ phase usually only occurs over a small temperature range, typically about 1 °C. Due to this narrow range, structural studies of the phase, have proven difficult. However, by broadening the $\text{SmC}^*_{\text{FI1}}$ phase using a highly chiral dopant, resonant x-ray scattering [12] was recently used to study this phase in more detail [10].

Recent theoretical work has shown that we can accurately reproduce experimental phase diagrams of materials that display the intermediate phases by minimizing the free energy of the system [13–16]. Although theoretically the stability of the smectic- C^* subphases can be predicted, why certain phases are exhibited in particular materials, and the driving forces behind their stabilization, is still not fully understood.

Bulk chirality and molecular shape are two factors which may contribute to the stability of the $\text{SmC}^*_{\text{FI1}}$ phase. Work on racemic mixtures in the various SmC^* subphases has been previously investigated [17] and Cady *et al.* [18] recently showed by ellipsometry that decreased enantiomeric excess has the effect of destabilizing the different intermediate phases. In order to study the effect of these two parameters on phase stability a pure compound exhibiting the intermediate phases may be doped with another liquid crystal molecule. Recent work showed that by doping a material exhibiting the $\text{SmC}^*_{\text{FI1}}$ phase with a highly chiral material (not liquid crystalline) of the same handedness, the $\text{SmC}^*_{\text{FI1}}$ and SmC^*_A phases are broadened significantly [10,19]. This fascinating observation demonstrated the potential sensitivity of the SmC^* subphases to chiral dopants and therefore to changes in bulk chirality. To date the $\text{SmC}^*_{\text{FI1}}$ and $\text{SmC}^*_{\text{FI2}}$ phases have only been observed in chiral systems, although we clearly cannot rule out other factors as the majority of materials do not exhibit these phases and some display one phase and not the other. Even more interestingly it was verified by resonant x-ray diffraction by the same group that the original $\text{SmC}^*_{\text{FI1}}$ phase in the host material was transformed to the $\text{SmC}^*_{\text{FI2}}$ phase on addition of the chiral dopant.

In this paper, we investigate the effects of mixing a host material with a rich smectic phase sequence with two different molecules. The first is a chiral molecule with the same chemical structure as the host material but with opposite-handed chirality. The second is the smaller achiral molecule, 8CB. Using these two mixture systems, we investigate independently both steric and chiral effects on the phase sequence of the host material. In particular we are interested in the effects of these two dopants on the three-layer intermediate phase ($\text{SmC}^*_{\text{FI1}}$).

II. EXPERIMENTAL METHODS

The host material used, AIS178, is an S-handed chiral molecule which exhibits four liquid crystalline phases [Fig. 2(a)]. This material has been studied by several different groups in recent years [2,8,19] and was in fact the main material used to determine the clock structure of the $\text{SmC}^*_{\text{FI1}}$ phase. The chiral dopant AIS174 has the same chemical structure and displays the same phases as AIS178 [Fig. 2(b)], but AIS174 is a right-handed chiral molecule. Both materials display a melting point at around 67 °C and extremely similar transition temperatures [Figs. 2(a) and 2(b)]. By doping

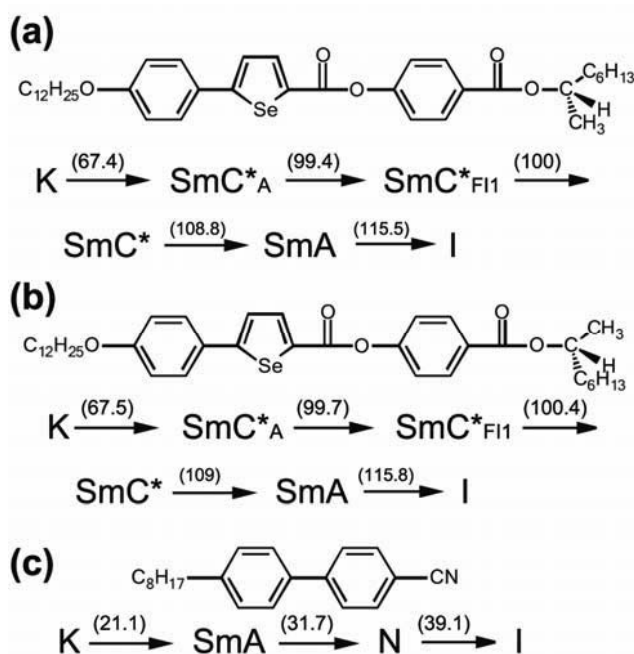


FIG. 2. Chemical structures and phase sequences of (a) AIS178, (b) AIS174, and (c) 8CB.

AIS178 with AIS174 the only property changed is the overall chirality of the mixture. In doping AIS178 with 8CB [Fig. 2(c)]: a shorter, achiral molecule, steric effects on the $\text{SmC}^*_{\text{FI1}}$ phase can be examined. 8CB is a simpler material, exhibiting only two liquid crystal phases, with a much lower melting point of 21 °C. Both AIS174 and AIS178 were synthesized in the Hird group at the University of Hull, UK, while the 8CB was purchased from Frinton Laboratories, Inc. (NJ, USA).

All the mixtures of AIS178 were prepared by varying the dopant concentration according to mass. Mixtures containing up to 30% 8CB were prepared, as the $\text{SmC}^*_{\text{FI1}}$ phase disappeared at fairly low concentrations of 8CB. Since AIS178 and AIS174 have similar phase sequences, and both display the $\text{SmC}^*_{\text{FI1}}$ phase, a full range of mixtures, from 0 to 100% AIS174, were studied. Mixtures were prepared by cycling the materials between states for an hour, heating them to the isotropic phase for five minutes and cooling to a liquid crystalline state for another five. Care was taken to ensure that all mixtures prepared were very well mixed. This was verified by both calorimetry measurements, producing a clear, single phase sequence, and by polarized optical microscopy.

Differential scanning calorimetry (DSC), using the Perkin-Elmer Diamond DSC system with a sample mass between 1 and 14 mg, was used to determine the transition temperatures of the mixtures. All DSC scans were run at the same rate of 7 °C/min and all reported transition temperatures are for heating runs, to avoid any effects of supercooling. Optical polarized microscopy, using a Leica microscope and a 10× objective lens, was used to identify the different liquid crystal phases in between transitions. Optical microscopy was also used to confirm the existence of the $\text{SmC}^*_{\text{FI1}}$ phase in mixtures with lower dopant concentrations, and to determine the phase widths of the $\text{SmC}^*_{\text{FI1}}$ phases, as the

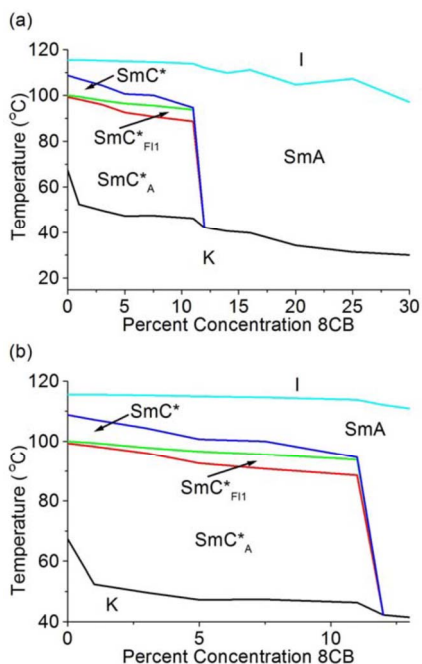


FIG. 3. (Color online) (a) Phase diagram of AIS178 with increasing 8CB dopant concentration. (b) Larger view of the same phase diagram highlighting the SmC^* subphases of the AIS178/8CB mixtures.

DSC peaks to and from this phase are small, on the order of background noise levels for the DSC instrument. Liquid crystal samples were placed between a clean glass slide and a cover slip and set on a Linkam LTS350 temperature stage for optical microscopy measurements.

Small angle x-ray scattering (SAXS) data was taken on the X6B beam-line at the National Synchrotron Light Source at Brookhaven National Laboratory, to determine the smectic layer spacing of the materials as a function of temperature. The X6B beam-line was configured to have a fairly small beam-spot size at the sample (0.2×0.3 mm), and a wavelength of 1.24 \AA . Additional SAXS data was taken at the x-ray crystallography facility (XRF) at the Institute of Molecular Biophysics at Florida State University. The XRF beam-line was configured with a slightly larger beam-spot size at the sample (0.5×0.5 mm), and a wavelength of 1.54 \AA . SAXS data was collected for the pure host material AIS178, the 7.5 and 11 % 8CB mixtures, and the 10 and 30 % AIS174 mixtures. X-ray data was taken from at least 30°C below the transition temperature to the smectic-A phase up to a few degrees above the transition point.

For layer spacing measurements the liquid crystal samples were contained between two sheets of Mylar and clipped onto a heating stage with a temperature stability of $\pm 0.1^\circ\text{C}$, ensuring good thermal contact. SAXS data was also taken for two pieces of Mylar without any liquid crystal between them to obtain scattering data from the Mylar, as well as any background scattering. Before analyzing the SAXS data of the mixtures, the data was normalized and the normalized empty Mylar data was subtracted.

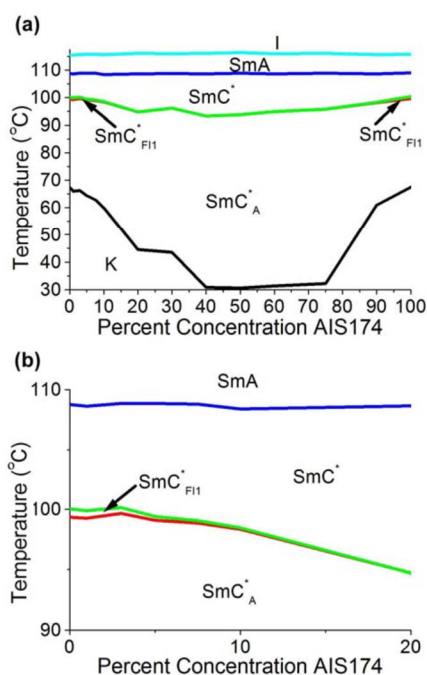


FIG. 4. (Color online) (a) Phase diagram of AIS178 with increasing AIS174 dopant concentration. (b) Larger view of the SmC^* subphases in the same phase diagram.

III. RESULTS

The DSC and optical microscopy data were combined to produce phase diagrams for the two sets of mixtures as a function of dopant concentration (Figs. 3 and 4). As can be seen in the AIS178/8CB phase diagram [Fig. 3(a)], the clearing and melting points behave as expected, decreasing with increasing dopant concentration. Looking more closely at the SmC^* subphases [Fig. 3(b)], the $\text{SmC}^*_{\text{F11}}$ phase width clearly increases with increasing 8CB concentration in the mixtures. Starting with a range of 0.6°C in the pure compound AIS178, this phase reaches a maximum width of 5.2°C at 11% 8CB, before completely disappearing, along with all other SmC^* subphases, at 12% 8CB.

For the AIS178/AIS174 phase diagram [Fig. 4(a)] the transitions to the isotropic and SmA phases hardly change with varying dopant concentration, while the SmC^* phase broadens a little. The phase diagram is symmetrical, with the $\text{SmC}^*_{\text{F11}}$ phase disappearing on addition of small amounts of the opposite-handed chiral material [Fig. 4(b)] and vanishing by 20% AIS174 dopant concentration. As can be seen in the phase diagram, the melting point decreases significantly with decreasing enantiomeric excess.

The DSC data for the 8CB mixtures show a clear peak at the SmA to isotropic (*I*) transition, which exhibits significant broadening with increasing achiral dopant (8CB) concentration [Fig. 5(a)]. Looking at the full-width at half-maximum (FWHM) of the SmA to *I* transition DSC peak as a function of dopant concentration [Fig. 5(c)] the peak visibly widens with increasing 8CB. In contrast when we compare the same transition peak for mixtures prepared with the chiral dopant (AIS174) the DSC peaks show no such widening [Figs. 5(b)

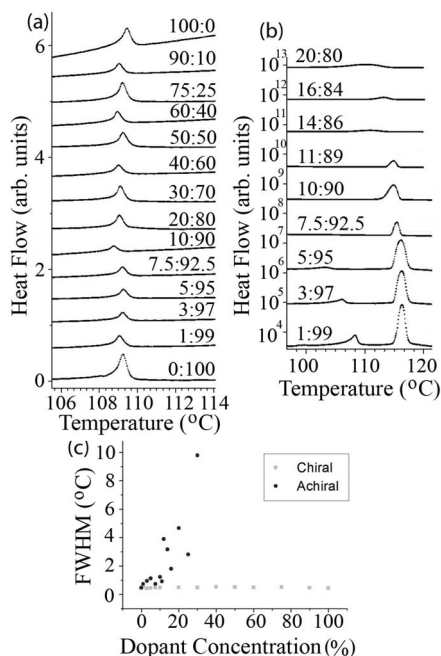


FIG. 5. DSC data for (a) 8CB mixtures and (b) AIS178 mixtures with ratio of dopant to AIS178 concentration given for each scan. (c) FWHM of the SmA to *I* peak in the two sets of mixtures.

and 5(c)]. Although a range of different sample masses were used, no correlation exists between the mass of the sample and the width of the peak.

Smectic layer spacing (*d* spacing) measurements are presented in Fig. 6 as a function of reduced temperature from the SmA phase and display characteristic behavior for the pure AIS178 and all mixtures studied using x-ray scattering, the 7.5 and 11% 8CB mixtures and the 10 and 30% AIS174 mixtures. The *d* spacing first decreases a little with increasing temperature, then increases significantly, 1–2 Å, over about 10 °C (Fig. 6) before becoming fairly constant, indicating a change from the SmC* phase to the SmA phase.

The 7.5% 8CB *d* spacing data [Fig. 6(b)] shows a discontinuity in the *d* spacing behavior about 20 °C below the transition temperature. This behavior consists of an increase in *d* spacing followed by an abrupt decrease in *d* spacing, right around the transition to the SmC*_{F11} phase. Smaller changes can also be seen in the pure AIS178, 11% 8CB and the 10% AIS174 mixtures, all near the transition temperatures to the SmC*_{F11} phase. This observation is consistent with recent work by Panov *et al.* [20] in which layer spacing discontinuities are observed at the smectic-C* subphase transition points by an optical film thickness measurement technique. These discontinuities are attributed to abrupt changes in the molecular tilt angle at the transition points.

Another discontinuity is seen in the 11% 8CB mixture [Fig. 6(c)], in which there is a sharp decrease (0.3 Å) in the layer spacing at the transition to the SmA phase. A discontinuity of 1 Å has been seen before in a different material [21] at the transition to an unidentified isotropic phase. This unidentified phase is believed to be highly twisted, possibly a smectic blue phase, thus leading to a smaller layer spacing. The texture of the 11% 8CB mixture above the transition

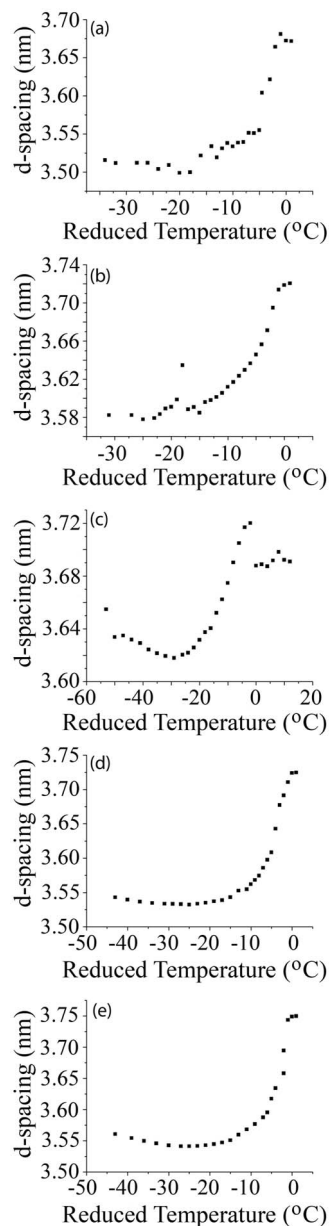


FIG. 6. Smectic layer spacing (*d*) versus reduced temperature from the SmA phase for the (a) pure AIS178, (b) 7.5% 8CB, (c) 11% 8CB, (d) 10% AIS174, and (e) 30% AIS174 mixtures.

temperature looks like that of the SmA phase, but as the layer spacing decreases suddenly at the transition to this phase more detailed studies need to be done to verify if this phase is indeed the SmA phase or a different, highly twisted phase.

Pure AIS178 has a *d* spacing which varies by 1.82 Å over the smectic phase range, while the 7.5% 8CB has a maximum change of 1.43 Å and the 11% 8CB mixture has a maximum change of 1.02 Å. With increasing amounts of the smaller, achiral molecule the variance in *d* spacing decreases. For the AIS174 mixtures, the 10% has a maximum change in *d* spacing of 1.92 Å while the 30% AIS174 has a maximum change of 2.09 Å. Despite the fact that AIS174 is the same size and shape of AIS178, with increasing amounts of this opposite-handed chiral dopant the change in *d* spacing increases. Addition of AIS174 also increases the *d* spacing

overall, with a maximum d spacing of 36.8 Å in the pure AIS178, 37.2 Å in the 10% AIS174, and 37.5 Å in the 30% AIS174. With the 8CB mixtures, the d spacing first increases, with a maximum d spacing of 37.2 Å in the 7.5% 8CB, and then stays the same for the 11% 8CB. All d spacing data has an error of about ± 0.2 Å, so the differences in maximum d spacing between mixtures are minimal when error is taken into account, although the difference in the maximum change in d spacing is significant.

IV. DISCUSSION

It is clear from this study that both steric and chiral effects are important in the stability of the $\text{SmC}^*_{\text{F11}}$ phase. Steric effects first stabilize this phase significantly, increasing the phase width by 4.6 °C, before destabilizing it, and all other SmC^* subphases, at a critical achiral dopant concentration between 11 and 12% for the 8CB dopant. Small amounts of opposite-handed chiral dopant, with the same molecular structure as the host material cause the $\text{SmC}^*_{\text{F11}}$ phase to shrink in width and then disappear, between 10 and 20% concentration. Since both the achiral and chiral dopants cause the $\text{SmC}^*_{\text{F11}}$ phase to destabilize near the same concentration, it is hard to tell from this experiment if steric or chiral effects play a more significant role in the stability of the $\text{SmC}^*_{\text{F11}}$ phase. Although it should be noted that the percentage concentrations used in this paper are measured by mass and do not take into account the differences in molar mass between materials. 8CB is a much smaller molecule (MW=291.43 g/mol) than AIS174 (MW=695.84 g/mol), therefore at a given percentage of dopant there will be 2.4 times more 8CB molecules in the mixture than AIS174 molecules.

Looking at recent research with a same-handed chiral dopant [19], only a 3% dopant concentration causes the $\text{SmC}^*_{\text{F11}}$ phase to change to a $\text{SmC}^*_{\text{F12}}$ phase. Also, the same-handed chiral dopant broadens this phase by over 20 °C. We observe that an achiral dopant broadens the $\text{SmC}^*_{\text{F11}}$ phase by approximately 5 °C, thus indicating that chiral effects play more of a role in the stability of the intermediate phases than steric effects. Steric effects do affect the range of temperatures over which a transition occurs, causing a broadening in the DSC peaks. This is expected, as there are competing effects between the chiral and achiral molecules due to their different preferred phases. The 8CB tries to be in the nematic or smectic-A phase while the AIS178 induces the smectic-C* subphases.

Looking at chiral effects, they clearly modify the melting point of the material. Since there is one minimum melting

point, and this melting point increases from the racemic mixture with additions of either enantiomer, we can surmise that the mixtures are racemic conglomerate: the two chiral species are well mixed but molecules of the same handedness tend to group together into nanodomains.

All of the mixtures which display the $\text{SmC}^*_{\text{F11}}$ phase exhibit a slight increase in d spacing around the transition temperature to the $\text{SmC}^*_{\text{F11}}$ phase, while the 30% mixture, which does not display the $\text{SmC}^*_{\text{F11}}$ phase, does not. This suggests a connection between the two. Since this change is much smaller in the 10% AIS174 mixture than in the 7.5% 8CB mixture and the range over which the $\text{SmC}^*_{\text{F11}}$ phase occurs is also much smaller in these materials, this further suggests that the $\text{SmC}^*_{\text{F11}}$ phase is the cause of the d spacing increase. However, the disruption in the 11% 8CB is also much smaller than in the 7.5% 8CB mixture, but the range of the $\text{SmC}^*_{\text{F11}}$ phase is actually larger in the 11% mixture, indicating that another mechanism may be behind the discontinuity in the d spacing data. The change in d spacing over the mesophase range decreases with increasing amounts of the achiral 8CB dopant. This indicates that the smaller molecules pack with the AIS178 in such a way as to reduce the tilt angle of the pure AIS178 molecule, which contributes to the increase in the overall d spacing of the 8CB mixtures. In contrast, the change in d spacing over the phase range increases with increasing AIS174 dopant [Figs. 6(d) and 6(e)]. The absolute value of the smectic layer spacing actually increases with increasing 8CB at any given temperature. This phenomenon is most likely due to suppression of AIS178 alkyl chain interdigitation by the shorter molecule. A similar effect is observed when the opposite handed AIS178 and AIS174 are mixed. As the overall d spacing is slightly increased for both dopants, this suggests that both the 8CB and the AIS174 molecules disrupt the closer packing that pure AIS178 molecules have, thus leading to wider layers.

ACKNOWLEDGMENTS

This work was supported by MARTECH, the Center for Materials Research and Technology, Florida State University and the Florida State University Council for Research Creativity. Dr. Helen Gleeson (University of Manchester, UK) kindly provided the chiral materials used in this experiment, which were synthesized by Dr. Michael Hird at Hull University, UK. Use of the National Synchrotron Light Source, Brookhaven National Laboratory, was supported by the U.S. Department of Energy, Office of Science, Office of Basic Energy Sciences, under Contract No. DE-AC02-98CH10886.

-
- [1] H. Takezoe and Y. Takanishi, in *Chirality in Liquid Crystals*, edited by H.-S. Kitzerow and C. Bahr (Springer, New York, 2001).
- [2] L. S. Hirst, S. J. Watson, H. F. Gleeson, P. Cluzeau, P. Barois, R. Pindak, J. Pitney, A. Cady, P. M. Johnson, C. C. Huang, A.-M. Levelut, G. Srajer, J. Pollmann, W. Caliebe, A. Seed, M.

- R. Herbert, J. W. Goodby, and M. Hird, *Phys. Rev. E* **65**, 041705 (2002).
- [3] J. P. F. Lagerwall and F. Giesselmann, *ChemPhysChem* **7**, 20 (2006).
- [4] T. Matsumoto, A. Fukuda, M. Johno, Y. Motoyama, T. Yui, S. Seomun, and M. Yamashita, *J. Mater. Chem.* **9**, 2051 (1999).

- [5] V. G. Chigrinov, *Liquid Crystal Devices: Physics and Applications* (Artech-House, Boston, 1999).
- [6] S. Inui, N. Iimura, T. Suzuki, H. Iwane, K. Miyachi, Y. Takanishi, and A. Fukuda, *J. Mater. Chem.* **6**, 671 (1996).
- [7] J. M. Oton, X. Quintana, P. L. Castillo, A. Lara, V. Urruchi, and N. Bennis, *Opto-Electron. Rev.* **12**, 263 (2004).
- [8] P. Mach, R. Pindak, A. M. Levelut, P. Barois, H. T. Nguyen, H. Baltes, M. Hird, K. Toyne, A. Seed, J. W. Goodby, C. C. Huang, and L. Furenid, *Phys. Rev. E* **60**, 6793 (1999).
- [9] P. M. Johnson, D. A. Olson, S. Pankratz, T. Nguyen, J. Goodby, M. Hird, and C. C. Huang, *Phys. Rev. Lett.* **84**, 4870 (2000).
- [10] N. W. Roberts, S. Jaradat, L. S. Hirst, M. S. Thurlow, Y. Wang, S. T. Wang, Z. Q. Liu, C. C. Huang, J. Bai, R. Pindak, and H. F. Gleeson, *Europhys. Lett.* **72**, 976 (2005).
- [11] A. Cady, J. A. Pitney, R. Pindak, L. S. Matkin, S. J. Watson, H. F. Gleeson, P. Cluzeau, P. Barois, A.-M. Levelut, W. Caliebe, J. W. Goodby, M. Hird, and C. C. Huang, *Phys. Rev. E* **64**, 050702(R) (2001).
- [12] H. F. Gleeson and L. S. Hirst, *ChemPhysChem* **7**, 321 (2006).
- [13] M. Čepič, E. Gorecka, D. Pocięcha, B. Žekš, and H. T. Nguyen, *J. Chem. Phys.* **117**, 1817 (2002).
- [14] A. Roy and N. V. Madhusudana, *Europhys. Lett.* **36**, 221 (1996).
- [15] E. Gorecka, D. Pocięcha, M. Čepič, B. Žekš, and R. Dabrowski, *Phys. Rev. E* **65**, 061703 (2002).
- [16] M. B. Hamaneh and P. L. Taylor, *Phys. Rev. E* **72**, 021706 (2005).
- [17] A. Fukuda, Y. Takanishi, T. Isozaki, K. Ishikawa, and H. Takezoe, *J. Mater. Chem.* **4**, 997 (1994).
- [18] A. Cady, Z. Q. Liu, X. F. Han, S. T. Wang, M. Veum, N. Janarthanan, C. S. Hsu, D. A. Olson, and C. C. Huang, *Phys. Rev. E* **66**, 061704 (2002).
- [19] S. Jaradat, N. W. Roberts, Y. Wang, L. S. Hirst, and H. F. Gleeson, *J. Mater. Chem.* **16**, 3753 (2006).
- [20] V. P. Panov, J. K. Vij, Y. P. Panarin, C. Blanc, V. Lorman, and J. W. Goodby, *Phys. Rev. E* **75**, 042701 (2007).
- [21] I. Nishiyama, J. Yamamoto, J. W. Goodby, and H. Yokoyama, *J. Mater. Chem.* **12**, 1709 (2002).